International Journal of Technology (2017) 4: 572-581
ISSN 2086-9614

ELECTROLYTIC REFINING OF LEAD IN MOLTEN CHLORIDE ELECTROLYTES

Pavel Arkhipov[1*], Yuriy Zaykov[1], Yulia Khalimullina[1], Anna Kholkina[1,2]

[1] *Institute of High Temperature Electrochemistry, Ural Branch, Russian Academy of Sciences, 20 Academicheskaya Street, Ekatherinburg, Russian Federation, 620990*
[2]*Ural Federal University named after first president of Russia B.N. Eltsin, 19 Mira Street, Ekatherinburg, Russian Federation, 620002*

(Received: October 2016 / Revised: May 2017 / Accepted: July 2017)

ABSTRACT

Three types of antimony and bismuth electrolytic cells to be used for lead electrorefining were developed and tested. The electrolytic cell with the bipolar metallic electrode, the electrolytic cell with two anodes and one cathode, and the electrolytic cell with the porous diaphragm were studied. The tests demonstrated that lead is effectively separated from the metallic impurities in all constructions. Grade lead may be obtained at the cathode, and lead-antimony and lead-bismuth alloys may be produced at the anode. The electrolytic cell with a porous diaphragm was found to double the production rate and greatly decrease the electrical potential of the cell as compared to the other two constructions.

Keywords: Antimony; Bismuth; Electrolytic cell; Electrolytic refining; Lead

1. INTRODUCTION

Battery scraps and other materials that contain a significant amount of lead oxides and sulfates may be recycled in gas-supplied furnaces under a reducing atmosphere at temperatures above 900ºC (Bredikhin et al., 2005). Lead with a small antimony concentration, slag containing to up 80% Pb and 10% Sb, and refractory films that appear at the surface of the melt are the products of reverberatory melting of the battery scrap without the addition of any reducing agents. However, a significant amount of lead, especially antimony, evaporates; hence, a possible extraction of lead may reach 95% at 5% gas losses. Many plants around the world use secondary materials for lead production, and reverberatory furnaces are primarily applied to melt lead loads with high oxides and antimony concentrations (Morachevsky, 2009). Both reverberatory melting and melting in shaft furnaces are ecologically unfriendly. Melting lead containing fractions in tubular rotatory furnaces operating in periodic regimes is mainly used in Europe. These furnaces allow the use of diverse types of fuel; recycle loads of intermediate composition; and require simple implementation, which makes them basic melting devices for small and medium enterprises. Rotatory furnaces were found to be of great convenience and are used worldwide as unique furnaces for single-phase lead melting and as auxiliary furnaces for a first stage slag depletion in, for example, Ausmelt slag furnaces (Tarasov, 2003). The slag may be recycled (James, et al., 2017).

Currently, there are several basic stages in industrial lead refining, including load preparation, reduction melting, and the subsequent removal of impurities in boilers; extraction of copper;

* Corresponding author's email: pavelarh@mail.ru, Tel. +7-343-2623462, Fax. +7-343-2623462
Permalink/DOI: https://dx.doi.org/10.14716/ijtech.v8i4.9473

oxidation refining from antimony, arsenic, and tin; desulphurization; the removal of bismuth; and alkali refining from calcium, magnesium, antimony, and zinc (Bredikhin et al., 2005). The required quality of the end product defines the duration, complexity, and power consumption when removing impurities. Thus, it is beneficial to produce lead of C2, C1 grades, per GOST standard 3778-98. The development of the nuclear industry will soon result in a growing demand for pure lead and Pb-Bi alloys to be used as liquid metal heat carriers (Sahu et al., 2012). To produce C00, C000 grade lead, per GOST standard 22861-93, using the same methods mentioned above, the process becomes time-consuming, multi-staged, and expensive. This is why it is important to develop a new, more eco-friendly technology for waste refining. Electrochemical refining in molten salts is the alternative method of pure lead production (Arkhipov et al., 2013; Arkhipov et al., 2014). Technology development plays a significant role in achieving SDG targets (Berawi, 2017).

The Laboratory of Electrode Processes at the Institute of High Temperature Electrochemistry of the Ural Branch of the Russian Academy of Sciences (IHTE UB RAS) is carrying out a complex study of the scientific basics of the electrochemical technology of lead refining in molten chlorides. The physical-chemical properties of the equimolar KCl-$PbCl_2$ mixture (Efremov et al., 2010; Efremov et al., 2016), kinetics of electrode processes at lead ion electroreduction (Zaikov et al., 2010; Pershin et al., 2010), lead electrodissolution from its alloys (Zaikov et al., 2008), and the thermodynamics of ternary lead-antimony-bismuth alloys (Arkhipov et al., 2016) have been studied. The electrochemical separation of alloys with high-purity lead extraction was performed during the laboratory-scale tests (Zaikov et al., 2008; Zaikov et al., 2010).

The present work reports on the test run of the electrochemical technology of lead refining using the equimolar mixture of potassium and lead chlorides in the electrolytic cells with a current load of 100–500 A. Transition from the laboratory cell to the industrial electrolytic cell usually causes changes in the heat and electric fields, which greatly influences the hydrodynamic environment inside the high temperature device. To solve these problems, three different constructions of electrolytic cells were developed. The electrolytic cells' test benches with a current load of 300–500 A were fabricated, and technological tests were performed. The construction of the three cells are unique, and each have vital differences.

2. METHODOLOGY

2.1. Electrolytic Cell 1 with the Bipolar Metallic Electrode

Figure 1 demonstrates a test bench for lead electrolytic refining, which is a reservoir that runs across the electrolyte that is separated by a graphite division wall into the anode and cathode parts and across the metal into the anode, bipolar electrode, and cathode parts . The graphite division wall is screened from the cathode side. The anode and cathode electrolytes have electrical contact via the bipolar liquid metal electrode. A graphite current lead and copper busses connect the anode metal and the direct current positive pole. The direct current negative pole is connected to the cylindrical graphite cathode via copper busses.

The walls of the electrolytic cell are made of fireproof concrete fabricated from corrosion-resistant high-alumina cement and fire clay chip. The wall thickness is over 200 mm. The cell is coated with a metallic sheath made of 10-mm-thick steel sheet.

To prepare the electrolyte, we used pure potassium chloride, per TR 2184-072-00209527, and pure lead chloride, per GOST standard 4210-77. Materials were first dried for 8 hours at 650 K. Then, the electrolyte was prepared according to its relation with metal chlorides in a weight ratio of mKCl:mPbCl2=1:2.5. Black lead, which was poured into 20 kg ingots and cut into 1 kg portions, was used as the anode metal.

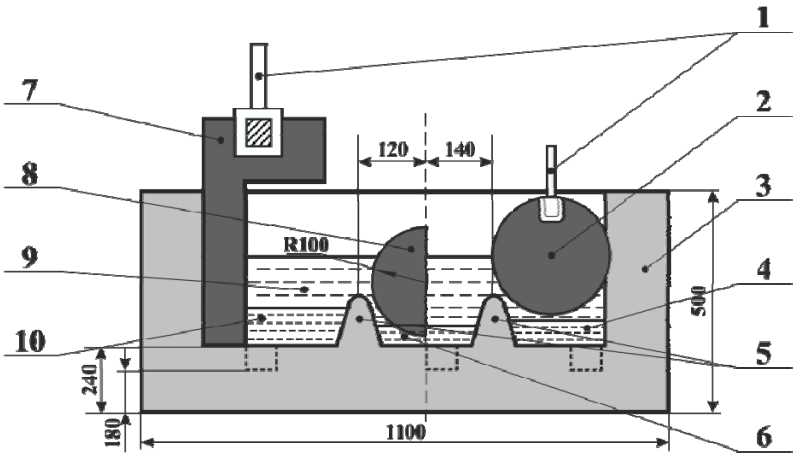

1 - current leads to electrodes;
2 - cathode;
3 - electrolytic cell body made of cement;
4 - cathode lead;
5 - division walls made of cement;
6 - bipolar electrode;
7 - anode;
8 - graphite;
9 - electrolyte;
10 - raw material.

Figure 1 Schematic of electrolytic cell 1 with the bipolar metallic electrode

The lining was dried by a nickel-chromium heater with an automatic temperature control mode that was installed into the anode and cathode areas. Both areas were heated over 10 days; the lining temperature was increased stepwise from 603 to 653 K; the exposure time was 10 days at 853 K. After drying, the heater was removed from the electrolytic cell. The reservoirs were filled with liquid lead of a C1 grade, and the KCl-PbCl2 mixture was loaded. The upper level of the melt was 150 mm above the metal's level. When the salts melted, the cell was heated by the electric current that flowed through the electrolyte.

When the desired amount of the refined lead was accumulated, the cathode metal was removed, and the anode alloy was added. Sampling of the anode and cathode alloys and the electrolyte was performed daily. The metal was analyzed using the Spektrolab-M device.

At start of the cell, 100 kg of electrolyte were loaded into the anode and cathode areas. The total level of the melt and metal was 22 cm in each reservoir. The molten KCl-PbCl2 mixture wetted out the material of the electrolytic cell and penetrated inside the pores. Thus, the lining was naturally impregnated with the electrolyte. The rate of the concrete impregnation was evaluated according to the electrolyte consumption per time unit at a constant level of the electrolyte in the anode and cathode areas. After 3 days, a permanent level of the melt in the electrolytic cell was set. Moreover, during the first day, the rate of the electrolyte impregnation into the lining pores was 20 kg/day, and during the second and third days, it was 11 kg/day.

2.2. Electrolytic Cell 2 with Two Anodes and One Cathode

To decrease the interelectrode distance and increase cell performance, the construction of an electrolytic cell with two anodes and one cathode was developed (see Figure 2).

Figure 2 illustrates the electrolytic cell, which is a reservoir divided by a graphite cathode across the electrolyte and by concrete barriers across the metal into two anode metal parts and a common cathode metal part. Graphite current leads and copper busses connect the anode metal and the direct current positive pole. The direct current negative pole is connected to the cylindrical graphite cathode located in the center of the cell via copper busses.

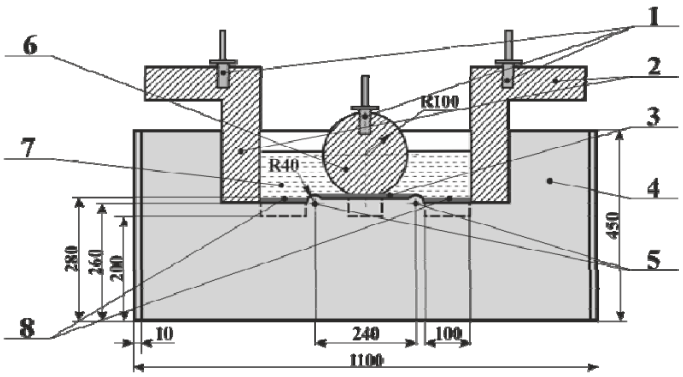

1 – current leads to electrodes;
2 – anodes;
3 – cathode lead;
4 – electrolytic cell body made of cement;
5 – division walls made of cement;
6 – cathode;
7 – electrolyte;
8 – raw material.

Figure 2 Schematic of the electrolytic cell 2 with two anodes and one cathode

Figure 2 illustrates the electrolytic cell, which is a reservoir divided by a graphite cathode across the electrolyte and by concrete barriers across the metal into two anode metal parts and a common cathode metal part. Graphite current leads and copper busses connect the anode metal and the direct current positive pole. The direct current negative pole is connected to the cylindrical graphite cathode located in the center of the cell via copper busses.

2.3. Electrolytic Cell 3 with a Porous Diaphragm

Porous ceramics may be used not only as filters (Nasir & Faizal, 2016), but as the electrolytic cell's construction material. Constructing the electrolytic cell with the porous ceramic diaphragm was done to provide a significant decrease in the interpolar distance (Figure 3). The set for the electrolytic refining of metallic lead contains a porous diaphragm (5) installed in the electrolytic cell body. This diaphragm is made in the form of a tank, where liquid metal is placed as one of the electrodes, which was the cathode in our case. Another electrode (anode) is located vertically around the diaphragm (5) in a ceramic crucible (4). The pores of the diaphragm walls are pointed from one wall to another. These pores are filled with the electrolyte and serve as a transport media for lead ions.

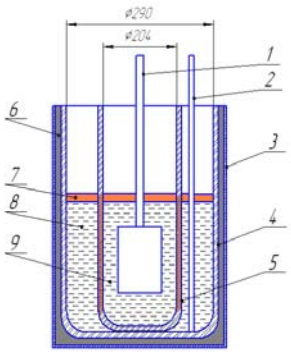

1 – cathode;
2 – anode;
3 – protective container (steel);
4 – ceramic crucible
6 – graphite powder;
7 – $PbCl_2$-KCl electrolyte;
8 – anode metal;
9 – cathode lead;

Figure 3 Schematic of the electrolytic cell 3 with the porous diaphragm

3. RESULTS AND DISCUSSION

3.1. Electrolytic Cell 1 with the Bipolar Metallic Electrode (Figure 1)

The technological processes in this device are as follows: black lead with impurities, wt.%: Sb: 1.0–2.0; Bi: 0.01–0.04; As: 0.005–0.02; Ag: 0.003; Sn: 0.002–0.003; Zn: 0.002–0.004 was loaded into the anode. The refining process was performed under the following technological parameters (Table 1).

Table 1 Technological parameters of electrolytic cell 1

Technological parameters	Value
Anode current density, A/cm^2	0.1–0.4
Cathode current density, A/cm^2	0.2–0.5
Total potential of the cell, B	12.0–16.0
Current load, A	300–500
Process temperature, K	803–823

First, lead and zinc ionization takes place at the anode that is under constant electric current, per the values of conventional standard potentials of metals:

$$Pb_{black} - 2e = Pb^{2+} \quad (1)$$

$$Zn_{black} - 2e = Zn^{2+} \quad (2)$$

and then the lead is reduced at the surface of the graphite division wall 7 (Figure 1):

$$Pb^{2+} + 2e = Pb \quad (3)$$

Lead, which is extracted at the graphite electrode, drains into the bipolar part. In addition, the metal surface in the medium part of the electrolytic cell acquires a positive value and transfers to the anode, where processes (1) and (2) proceed repeatedly, and process (3) takes place at the cathode. As the result of the electrolysis, lead passes from the anode to the cathode, and antimony, tin, copper, bismuth, and arsenic stay at the positive electrode, and their content in the anode alloy increases continuously. Zinc transfers to the chloride melt and remains there as the electrolyte compound.

During the refining, the antimony concentration in the cathode's metal decreased from 0.0007 to 0.001 wt.% and then remained constant at further electrolytic cell operation in the chosen mode. In addition, the impurities bismuth, arsenic, silver, calcium, and antimony accumulated in the anode metal.

During the tests, the antimony concentration in the anode alloy increased from 1 to 34 wt.%, whereas in the cathode melt, its concentration was four times lower. These data are supported by the theoretical calculations and laboratory tests. A test bench of cathode lead of C1 grade, per GOST 3778-98, was produced during the tests.

Experimental tests of this electrolytic cell's construction demonstrated that lead is effectively separated from metallic impurities. It is possible to obtain grade lead at the cathode and lead-antimony alloy at the anode. However, low-current densities make the process lengthy and show a high potential of the electrolytic cell, making the process energy consuming.

3.2. Electrolytic Cell with Two Anodes and One Cathode (Figure 2)

The electrolytic cell's body was made of fireproof cement, the same as the electrolytic cell described above. Lead-bismuth alloy with impurities wt.%: Bi: 1.6–1.7; Sb: 0.01–0.02; As: 0.003–0.004; Ag: 0.003 –0.01; Sn: 0.001 –0.002; Zn: 0.002–0.004 grinded into 1–2 kg pieces

was used as the anode metal. The alloy was loaded in portions to maintain the changes in metal levels within 1 cm.

The cathode's lead was removed periodically when the cathode tank became full or three times per day. per the theoretical calculations, by a special bucket and was then poured into an ingot; it was cooled and weighed. According to the weight of the cathode lead, the lead-bismuth alloy feed to the electrolytic cell anode area was defined. The quality control of the end products was performed by sampling the anode and cathode metals and electrolyte once a day.

The electrolytic cell was tested over a span of 14 days using the KCl-PbCl2 melt. The process conditions were defined for the laboratory-scale refining process (Table 2).

Table 2 Technological parameters of electrolytic cell 2

Technological parameters	Value
Anode current density, A/cm^2	0.2–0.35
Cathode current density, A/cm^2	0.35–0.7
Total potential of the cell, B	7.0–8.0
Current load, A	300–500
Process temperature, K	803–823

During the test, 192 kg of the lead-bismuth alloy were recycled. The test batch of 184 kg of the cathode lead was produced.

The tests results are provided in the form of a graph of the controlled impurities' concentration changes. Figure 4 demonstrates the time dependence of the metallic impurities' concentrations in the cathode metal.

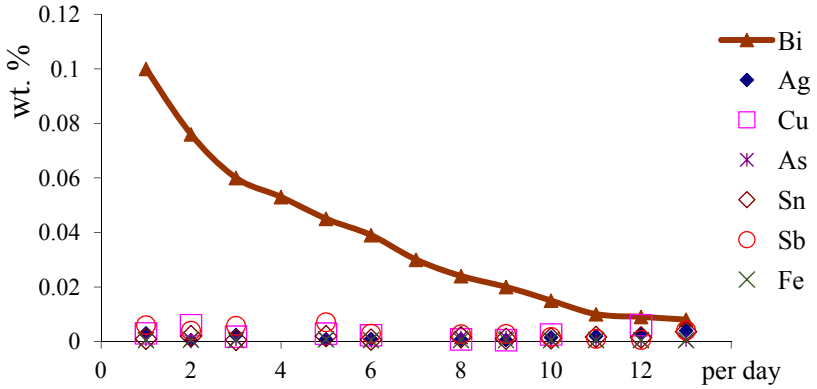

Figure 4 Time dependence of the metallic impurities' concentrations in the cathode metal

From Figure 4 demonstrates that the bismuth fraction in the cathode metal decreased from 0.1 to 0.01 wt.% during the refining process. The concentrations of the other impurities decreased and remained on the detection accuracy level. The behavior of copper in the cathode lead was peculiar; at the beginning of the experiment, its concentration decreased to 0.002 wt.% and remained constant.

Figures 5 and 6 illustrate the time dependencies of the metallic impurities' content in the anode metal.

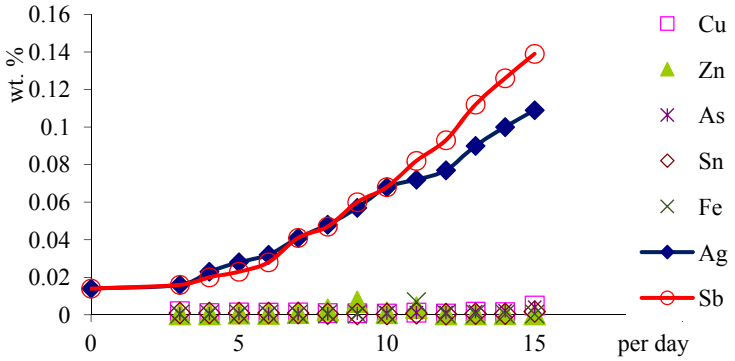

Figure 5 Time dependence of the metallic impurities' content in the anode metal

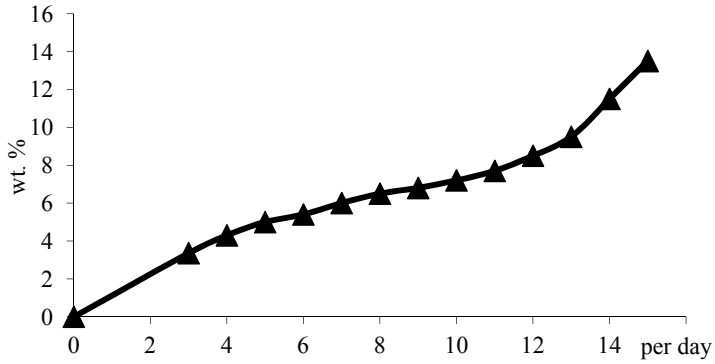

Figure 6 Time dependence of the concentration of bismuth in the anode metal

The According to Figures 5 and 6, impurities such as bismuth, antimony, and silver accumulated in the anode metal; the concentrations of other impurities increased to 0.005 wt.%. During the tests, the mass fraction of bismuth in the anode alloy increased from 1 to 14 wt.% (Figure 6); the concentration of bismuth in the cathode metal was three times smaller.

Experimental tests of the second electrolytic cell's construction demonstrated that the lead was effectively separated from metallic impurities as in the previously analyzed construction. Grade lead may be produced at the cathode, and lead-bismuth alloy may be obtained at the anode. The current densities were a little higher than in the first case, but the electrolytic cell's potential decreased two times at the same current load. The real value of the current density on separate parts of the liquid metal anode may differ from the values of the average current density, which were calculated for the whole geometric surface. Papers (Efremov et al., 2007; Efremov et al., 2012) have shown that the real value of current densities near the division barrier between liquid metal electrodes is several times higher than the calculated one. To provide the even distribution of the electrical field, power lines along the electrode's surface on the third electrolytic cell's construction was developed.

3.3. Electrolytic Cell 3 with Porous Diaphragm (Figure 3)

The refining process was performed under the following technological parameters (Table 3).

The total potential variations during the current load were negligible, per the level of anode and cathode metals. The values were 1.0; 1.3; 1.5; 2.1 V for the current densities of 0.3; 0.5; 0.7; 1.0 A/cm^2, respectively. Figure 7 illustrates the total potential variations of the electrolytic cell for the current density of 0.1 A/cm^2.

The maximums on the potential curve correspond to the cathode's lead removal. When the level of metal in the cathode part decreased, the current density increased, which resulted in the total

potential growth. The minimums of the potential curve correspond to the black lead feed into the anode.

Table 3 Technological parameters of the electrolytic cell 3

Technological parameters	Value
Anode current density, A/cm^2	0.3–1.0
Cathode current density, A/cm^2	0.3–1.0
Total potential of the cell, B	1.0–2.1
Current load, A	300–500
Process temperature, K	803–823

At each current density, the process was carried out over several days, uninterrupted.

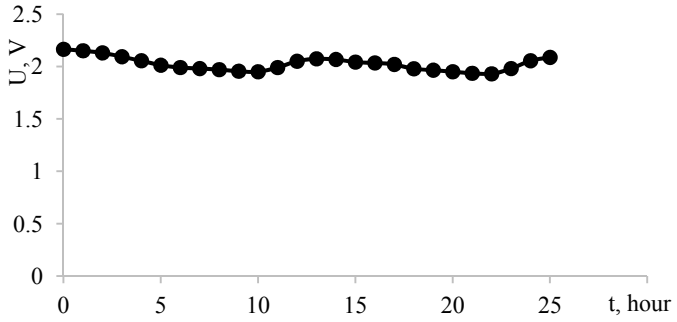

Figure 7 Time dependence of the total potential variation of the electrolytic cell at i=1.0 A/cm^2

The chemical compositions of the original lead feed and electrorefined cathode product at the current density of 1.0 A/cm^2 are presented in Table 4.

Table 4 Impurities concentrations in the raw material, anode metal, and electrorefined cathode product, wt.%

Metal	Sb	Sn	Cu	Zn	Bi	Fe	As	Ag	Pb
Raw material	2.06	0.002	0.02	0.0005	1.4	0.0055	0.12	0.12	Residual
Anode	11.8	0.005	0.043	0.0008	7.4	0.0059	0.6	0.6	Residual
Cathode	0.0001	0.001	0.01	0.001	0.0003	0.0006	0.0004	0.0006	Residual

The data presented in Table 4 show that the obtained cathode lead meets the requirements for grade lead and can be a commercial product. Table 5 presents a comparison of the technological parameters of the electrochemical refining process in the three electrolytic cells under study.

Table 5 Technological parameters of the electrolytic cells

Technological parameters	Cell 1	Cell 2	Cell 3
Anode current density	0.1–0.4	0.2–0.35	0.3–1.0
Cathode current density	0.2–0.5	0.35–0.7	0.3–1.0
Total potential of the cell	12.0–16.0	7.0–8.0	1.0–2.1

According to the test run of the electrochemical technology of lead electrorefining in the equimolar potassium and lead chloride mixture, the electrolytic cell with the porous diaphragm demonstrated the optimal parameters for pure lead production. For example, the upper limit of the cathode's current density (the process rate) of the third electrolytic cell (Figure 3) was three times higher than that of electrolytic cells 1 (Figure 1) and 2 (Figure 2). In addition, the total bath potential of electrolytic cell 3 (Figure 3) was four times lower than that of the electrolytic cell 2 (Figure 3) and eight times lower than that of the electrolytic cell 1 (Figure 1).

4. CONCLUSION

Three types of antimony and bismuth electrolytic cells to be used for lead electrorefining were developed and tested. The tests demonstrated that lead is effectively separated from the metallic impurities in all the constructions under study. Grade lead may be produced at the cathode, and lead-antimony and lead-bismuth alloys may be obtained at the anode. However, low-current densities of the first and second electrolytic cells make the refining process time-consuming, and the high potentials of the first and the second cells make the process costly because of the high power consumption. Therefore, the electrolytic cell with the porous diagram proved to be the most efficient for grade lead production in molten chlorides.

5. REFERENCES

Arkhipov, P., Kholkina, A., Zaykov, Yu., 2016. EMF Measurements in the Liquid Pb/PbCl2-KCl/Pb-Sb-Bi System. *Journal of Electrochemical Society*, Volume 163(2), pp. H30−H35

Arkhipov, P.A., Zaykov, Yu., Ashikhin V.V., Khalimullina, Yu., Tropnikov D.L., 2013. *Method of Electrolytic Lead Obtaining Pat. RF No 2487199*, issued 10.07.2013 (in Russian)

Arkhipov, P.A., Zaykov, Yu., Khalimullina, Yu., 2014. *Electrolyzer for Thin Layer Metallic Lead Electrolytic Refining Pat. RF No 2522920*, issued 21.05.2014 (in Russian)

Berawi, M.A., 2017. The Role of Technology in Achieving Sustainable Development Goals. *International Journal of Technology*, Volume 8(3), pp. 362−365

Bredikhin, V.N., Manyk N.A., Kaftanenko, A., 2005. *Secondary Lead. Donetsk: DONNTU*, pp. 131 (in Russian)

Efremov, A., Apisarov, A., Arkhipov, P., Zaikov, Yu., 2010. Electrical Conductivity and Liquidus Temperature of the Molten $PbCl_2$−KCl−PbO System. *The Melts*, Volume 1, pp. 29−34 (in Russian)

Efremov, A., Arkhipov P., Zaikov Yu., 2007. Constant Current Distribution Along the Liquid Metal Anode and in the $PbCl_2$–KCl Electrolyte Bulk. News of Higher Educational Institutions. *Ferrous Metallurgy*, Volume 3, pp. 12−19 (in Russian)

Efremov, A., Arkhipov, P., Zaikov, Yu., 2012. Electrical Field Modelling in the Liquid Metal Anode Electrolytic Cell. *The Melts*, Volume 5, pp. 37−42 (in Russian)

Efremov, A., Kulik, N., Kataev, A., Arkhipov, P., Redkin, A., Chuikin, A., Arkhipov, P., Zaikov, Yu., 2016. Electrical Conductivity and Liquidus Temperature of the EQUimolar KCl−$PbCl_2$ Mixture with Lead Oxide Additions. News of Higher Educational Institutions. *Ferrous Metallurgy*, Volume 5, pp. 10−16 (in Russian)

James, J., Lakshmi, S.V., Pandian, P.K., 2017. A Preliminary Investigation on the Geotechnical Properties of Blended Solid Wastes as Synthetic Fill Material. *International Journal of Technology*. Volume 8(3), pp. 466−476

Morachevsky, A.G., 2009. *Physical Chemistry of Lead Recycling*. Polytechnical University Publishing, St. Petersburg, Russia, pp. 271 (in Russian)

Nasir, S., Faizal, S., 2016. Ceramic Filters and Their Application for Cadmium Removal from Pulp Industry Effluent. *International Journal of Technology*, Volume 7(5), pp. 786−794

Pershin, P., Khalimullina, Yu., Arkhipov, P., Zaikov, Yu., 2014. The Electrodeposition of Lead in LiCl−KCl−$PbCl_2$ and LiCl−KCl−$PbCl_2$−PbO Melts. *Journal of Electrochemical Society*, Volume 161(14), pp. D824−D830

Sahu, S.K., Ganesan, R., Gnanasekaran, T., 2012. Studies on the Phase Diagram of Pb-Fe-O System and Standard Molar Gibbs Energy of Formation of '$PbFe_5O_{8.5}$' and $Pb_2Fe_2O_5$. *Journal Nuclear Materials*, Volume 426, pp. 214−222

Tarasov, A.V., 2003. *Metallurgical Refining of Lead Containing Secondary Materials*. Gintsvetmet, Moscow, Russia, pp. 223 (in Russian)

Zaikov, Yu., Arkhipov, P., Khalimullina, Yu., Ashikhin, V., 2008. Separation of Pb-Sb Alloys by in Molten Chloride. *The Melts*, Volume 6, pp. 59−63 (in Russian)

Zaikov, Yu., Arkhipov, P., Khalimullina, Yu., Ashikhin, V., 2010. Cathode Processes in KCL−$PbCl_2$ Melt. *In*: Proceedings of the 9th Israeli-Russian Bi-National Workshop, pp. 186−197

Zaikov, Yu., Arkhipov, P., Khalimullina, Yu., Ashikhin, V., Khramov, A., 2008. Anode Dissolution of Pb−Sb Alloys in the Equimolar Mixture of Potassium and Lead Chlorides. News of Higher Educational Institutions. *Ferrous Metallurgy*, Volume 4, pp. 11−18 (in Russian)

Zaikov, Yu., Arkhipov, P., Khalimullina, Yu., Skopov, G., Pershin, P., Kholkina, A., Molchanova, N., 2010. Anode Behavior of Pb-Bi Alloys in Molten Chlorides. *The Melts*, Volume 6, pp. 19−25 (in Russian)